3
Experimental Techniques

3.1 INTRODUCTION

Perovskite oxide films with better microstructures are preferable for applications such as ferroelectric random access memory (FeRAMs), frequency agile devices and electro-optics. The fabrication of high-quality crystalline and epitaxial oxide films with better dielectric properties favors of possible device scaling and integration with semiconductor technologies. The use of bulk material ceramic in tunable component was limited mainly because of very large required DC voltage in order to achieve good tunability. Hence thin films are found more attractive due to smaller in size, large number of integration and lower power requirement. There has been extensive research carried out on thin film based microwave tunable devices including tunable filters, voltage controlled oscillators. The properties of thin films depend on its real structure of a given material. There is correlation between parameters of thin film deposition and its functional properties. The engineering properties of a thin film can be facilitated by manipulating its film structure where film formation is considered as a starting process including nucleation followed by coalescence and finally growth of the film. When these target material species reach on the substrate surface, several physical processes are involved in their settlement there and the thin solid films are formed from the vapor phase by the nucleation and growth of individual islands/clusters. Real substrate surfaces, however, may be far from perfect with uneven surface, containing a distribution of kinks, dislocations and point defects [Noguera, 1996]. Binding of small clusters and single atoms on the substrate can be influenced by the imperfections and nucleation behavior is greatly affected on a perfect terrace. Therefore the surface states of the substrate have an important influence on the early stages of film growth.

Target atoms arrive at a rate dependent on the deposition parameters on a substrate surface and get adsorbed. The adsorbed atoms can subsequently diffuse on the substrate surface which also governed by substrate temperature. Thereafter these atoms can either re-evaporate or form clusters, depending on the bonding of atoms to the substrate and materials vapor pressure. The clusters, above the critical size are stable and metastable clusters may either diffuse to these stable clusters or dissociate. Further, the subsequent arriving single atoms can diffuse directly across the substrate to get attached to the stable cluster, or they can directly impinge on the grown clusters and get incorporated into them. The atoms can re-evaporate from the cluster or can detach from it and remain on the substrate surface. Total free energy of the cluster governs the balance between the growth and dissolution process for a given cluster, contrast to an assembly of individual atoms. The arriving target atoms of the film material can bind more loosely or strongly to the substrate atoms then to among themselves. The various processes involved in the formation (nucleation) of atom clusters by vapor deposition on a substrate are illustrated systematically in Figure 3.1.

The chemical potential from one monolayer to the next of the deposited film vary due to elastic strain. In considering the common theory of film nucleation and growth, there are three different conventional growth modes have been observed [van der Merwe *et al,* 1986].

(i) Two-dimensional full-monolayer growth (Frank-van der Merwe)
(ii) Two-dimensional growth of full monolayers followed by nucleation and growth of three-dimensional islands (Stranski-Krastinov)
(iii) Three dimensional island growth (Volmer-Weber)

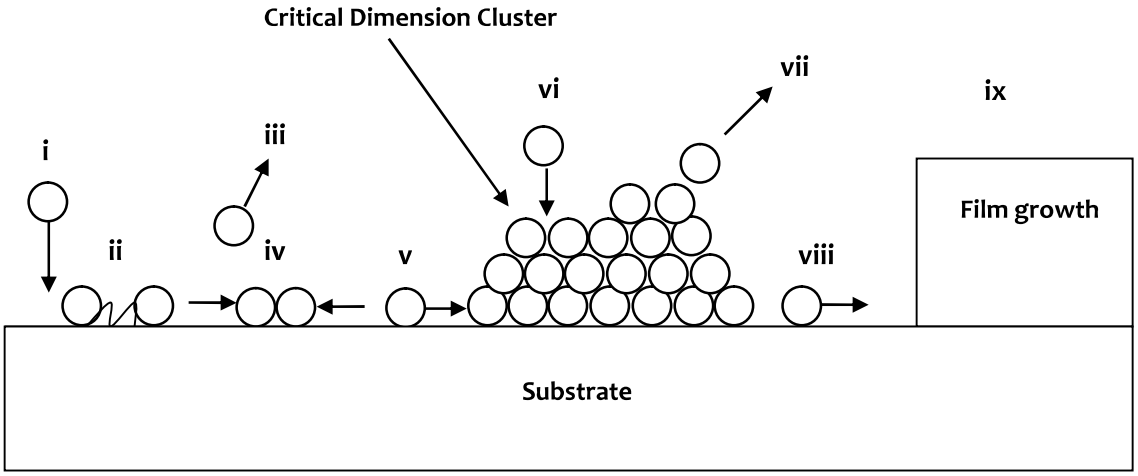

Figure 3.1: The Schematic diagram of the thin film growth process.
(i) Arrival of the material species near the substrate surface (ii) Accommodation of the arrived species on the substrate surface (iii) Re-evaporation from the substrate (iv) Metastable cluster nucleation (v) Diffusion to Critical size cluster (vi) Atom deposition on cluster (vii) Re-Evaporation from cluster (viii) Dissociation of cluster (ix) Film formation.

These three processes are schematically shown in Figure 3.2. The selection of any one of these growth modes depends on the surface and interface energies of the film and the substrate for a specific substrate-film system.

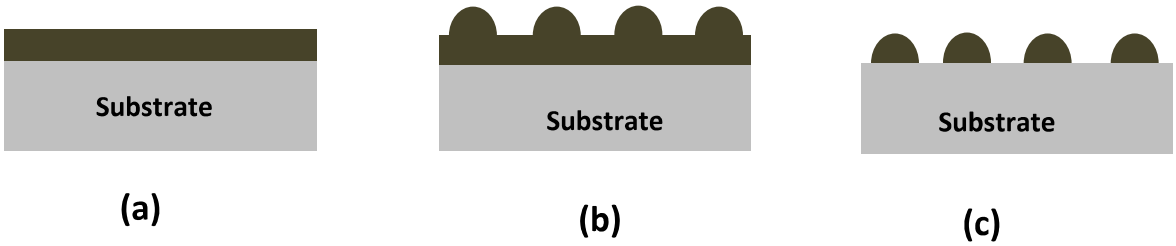

Figure 3.2: Schematic representation of the three conventional thin film growth modes: (a) layer or Frank-van der Merwe mode, b) layer plus island or Stranski-Krastanov mode and c) island or Volmer-Weber

The growth of the film depends on two competing forces. The forces are target film crystal structure and substrate crystal corresponding to preserve its own structure and to enforce its own structure onto the film respectively. The relative strength of these two competing forces govern final position of the film atoms via the relative bond strength, film substrate misfit, film thickness and the growth temperature. The deposition and growth rates are low enough in various film growth techniques and the relevant atomic processes are fast enough so that quasi-equilibrium dominates. The governing principle is the minimization of the free energy which strongly depends on the interface misfit. The growth modes also depend on the temperature and the deposition rate of the film. For a cluster that is large enough to be reasonably accepted as a continuum solid, its free energy can be given by Greene's notation, as follows:

$$\Delta G = a_1 r^2 \Gamma_{c-v} + a_2 r^2 \Gamma_{s-c} - a_2 r^2 \Gamma_{s-v} + a_3 r^3 \Delta G_V \tag{3.1}$$

where r is the radius of the cluster with area of surface $a_1 r^2$ in the vapor phase, a contact area $a_2 r^2$ with the substrate and a volume $a_3 r^3$; a_i's being the constants which depend on the nuclei shape. The Γ's are the interface energies between the condensate (c), substrate (s),

and vapor (v) phase, and ΔG_V is the change in free volume energy of the cluster on condensation. If, for a given cluster size, the derivative of this free-energy change in the cluster is positive with respect to the atoms, then the clusters of that size will shrink on average and the cluster is not stable. If this derivative is negative, then the clusters grow on average and that size cluster is stable. To a first approximation the free volume energy per unit volume on condensation of the cluster can be represented as

$$\Delta G_V = \frac{kT}{\Omega} \ln \frac{P}{P_e} = \frac{kT}{\Omega} \ln \zeta \tag{3.2}$$

where k is Boltzmann's constant, T is the absolute temperature, Ω is the volume of an adatom, P is the pressure of the arriving atoms, P_e is the equilibrium pressure of the film atoms, and ζ is the supersaturation. The free condensation of a cluster from a vapor is truly governed by this expression. For a pressure of arriving atoms the change in volume free-energy will be negative in excess of the equilibrium vapor pressure and will attain more negative values for increased supersaturation. Supersaturation can be increased by reducing substrate temperature and increased deposition. An expression for the critical cluster size r* can be obtained by maximizing ΔG in Eq. (3.2).

$$\frac{\partial(\Delta G)}{\partial r} = 0 \Rightarrow r^* = -\frac{2\Gamma_{c-v}}{\Delta G_V} \qquad \Delta G^* = \frac{16\pi\Gamma^3}{3(\Delta G_V)^2} \tag{3.3}$$

The variation of total change in free energy versus radius of the film nuclei is shown in Figure 3.3 along with the contribution of the free volume energy [Whatmore *et al,* 1999] and surface energy. The clusters with size less than r* will dissolve the growth, while clusters size larger than critical size r* will lower their free energy by continuing the growth.

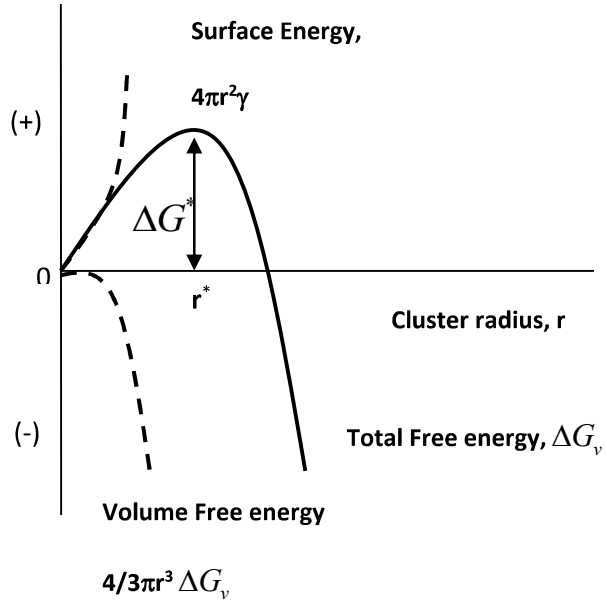

Figure 3.3: The variation of the free energy versus the radius of the film nuclei.

Full monolayer can be favored by low film surface energy, strong film-substrate bonding and high substrate surface energy for the deposition of the film on different materials as substrate. The nucleation and growth of islands still govern the 2D layer by layer growth, which are one unit cell thick and essentially coalesce completely before significant clusters are developed in next film layer. The atoms are bounded more strongly to the substrate than each other thereafter atoms condense first and formation of monolayer take place on the surface

which is covered with a less tightly bound second layer. Providing a decrease in binding which is monotonic, toward the bulk crystal of the deposit, the layer growth mode is initiated.

Smooth growth of the films is resulted from this mode with low density of structural defects. On the other hand in island, or Volmer-Weber mode (Figure 3.3(c)), small clusters are nucleated directly on the substrate surface and then grow into islands of condensed phase. More strongly binding of atoms to each other rather than substrate, favors for island growth. Different islands are characterized by different growth rates consequently give rise to rough surface. The layer plus island or Stranski-Krastanov (SK) growth mode (Figure 3.3 (b)) is an interesting intermediate case between the island and layer growth modes and occurs in a number of cases in which layer growth would depend on the surface energy grounds. It consists of initial 2D layer by layer growth with a subsequent transition to 3D-island growth. Initial deposition leading to the formation of expected one or more strained monolayers, whose structure is strongly subjected to the underlying substrate. After forming the first monolayer subsequent layer growth is unfavorable due to the strain at the interfaces of these layers and islands are formed on top of this layer. Three-dimensional islands nucleate and grow eventually after formation of adatom layer from further deposition. Deposition conditions and the substrate in the process govern structure, number of adsorbed layers, number density and shapes of the islands. Disturbance for the monotonic decrease in binding energy can be also reason to occurrence of this mode and characteristic of layer growth.

3.2 THIN FILM DEPOSITION TECHNIQUES

Sputter deposition is a general technique for the deposition of thin films, and is part of the Physical Vapor Deposition (PVD) group of methods, which also includes RF magnetron sputtering, Pulsed Laser Deposition (PLD), thermal evaporation and molecular beam epitaxy (MBE). Rresearch efforts have been undertaken on the growth of high quality ferroelectric thin films using a variety of deposition techniques including PLD, RF magnetron sputtering and MBE. However, MBE is just start to be considered for deposition of ferroelectric oxides, while sputtering and PLD have been extensively used for the growth. During the growth, the importance is given to encourage high quality growth and optimisation of deposition parameters.

3.2.1 RF Magnetron Sputtering

For many materials, sputtering deposition has been recognized as a technique which offers superior film properties (both structural and electrical) in comparison to other physical vapor-deposition techniques. This is especially evident in the use of sputtering for the hetroepitaxial growth of multicomponent metal oxides. These materials containing three or more different atomic species can be deposited in-situ as thin films, with the use of a sputtering to rapidly heat and evaporate a multicomponent metal oxide target. RF magnetron sputtering has been extensively accepted techniques for the deposition of better quality ferroelectric thin films by various research groups [Padmini *et al,* 1999; Im *et al,* 2002]. The reason for better choice as deposition has been considered due to sputtering of any solid material (metals, insulators and semiconductors) and complex compounds. The deposition can be performed stoichiometrically using low gas pressure with appreciable deposition rates and large area uniformity. The sputtering also promotes smoother surface, good adhesion and lower deposition temperature.

Sputtering is a PVD technique for thin film deposition which is performed in vacuum chambers and collision of plasma appears to eject material from target onto substrate. In sputtering, glow discharge plasma of molecules makes strike onto the target and eject out the atoms from target material. The sputtered atoms are not in thermodynamic equilibrium and deposited all around in sputtering chamber. The average of ejected atoms per incident ion is defined as sputter yield. The yield depends on the ion energy, ion incident angle, target atoms, masses of the ion and surface binding energy of atoms in target.

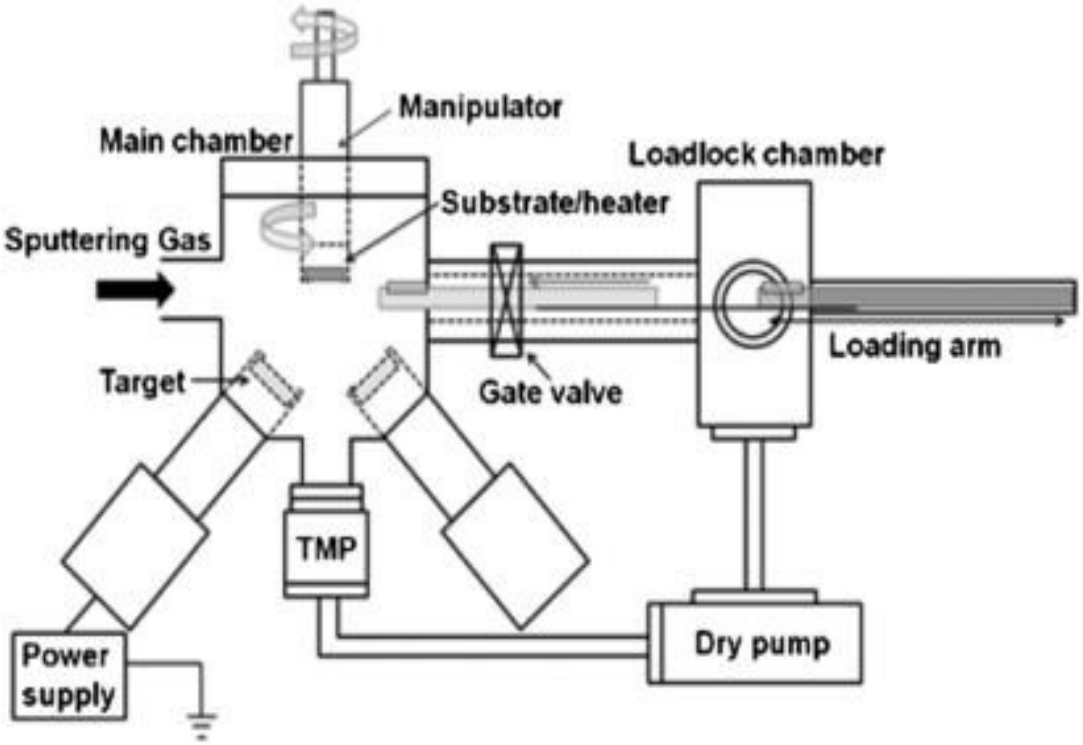

Figure 3.4: A schematic of the sputtering process.

The sputtering system is configured with a deposition chamber associated to a high vacuum pump. The sputtering target is placed on to a circular electrode inside the chamber, which acts as cathode and is mounted in front of substrate. Prior to the sputtering, chamber is evacuated to a high vacuum, to remove atmospheric gases leads to reduce contamination and unnecessary scattering. An inert gas is introduced and suitable pressure is to be maintained in the chamber which is ionized by a appropriate voltage applied between the two electrodes to generate glow discharge plasma [Rossnagel, 2002]. The high voltage between the cathode and the anode initiates plasma at pressures in the militorr (mTorr) range. The ions get accelerated causes to dislodge target atoms by bombardment of the target and get deposited on the anodic substrate. The target as cathode attracts positive ions and an energy transfer occurs when a positive ion collides with atoms at the solid surface. Primary recoil atoms can be generated when the transfer of energy to a lattice site is greater than binding energy. These primary atoms can collide to other atoms and distribute its energy through collision cascades. Inert gases produce a film of similar composition to the target while mixture of reactive and inert gases produces a film which is combination of the target species and reactive gas. Sputtering of a target atom is one of possible impact of ion bombardment while secondary electrons are emitted from ion bombardment apart from sputtering and sustains the plasma. Regardless of the specific method, the objective is to deposit a uniform, thin layer of the target composition on the substrate, replicating the close stiocheometry of the target material. High vacuum generation is normally a two stage process; low vacuum by roughing pump followed by high vacuum pump with switch to a longer pumping time. The roughing pump works as backing pump during the high vacuum pumping cycle, to achieve high vacuum and base pressure is achieved in the range of 10^{-6} to 10^{-8} Torr on most of the sputtering systems. Highly pure inert sputtering gas is inserted after achieving the desired base pressure. The sputtering gas pressure is regulated by a combination of gas flow process and throttling the high vacuum pump. It should be highlighted that the high vacuum pump is not entirely throttled during sputtering deposition while a steady gas flow is maintained in the chamber. There are numerous sputtering methods which includes DC sputtering, RF sputtering, and RF/DC magnetron

sputtering. RF sputtering is used for insulating materials, while conducting materials require a DC power supply. The deposition rate is promoted by introduction of magnetic field in RF magnetron sputtering.

The most commonly used configuration among the various available configurations, is magnetron sputtering with circular target. In the magnetron sputtering, charged particles are confined by the magnetic confinement and hence increasing ionization close to the target. The sputtered atoms are unaffected by the magnetic field because of neutrally charged atoms. In such a condition, ions are accelerated towards the target whereas the electrons are confined within the magnetic field lines. The magnetic field is placed parallel to the cathode in such a suitable orientation of the field polarity while keeping in mind that the secondary electrons must be confined within the drift loop. The probability for ionizing collisions increases with neutral atoms near the target by forming a helical path of the electrons around the magnetic field lines. The increased confinement produces high plasma density area close to the cathode for formation of high current discharge at low voltage. Due to the high plasma density, low operating pressures can be achieved which results into less gas scattering between the sputtered atoms and the chamber gas. The kinetic energy of the sputtered atom increases with reduced scattering which grow the atom transport to the substrate from the cathode. The high discharge current is produces to sputter cathode at a high rate and therefore higher deposition rates can be obtained. However cooling capability of the cathode is another limiting parameter for the maximum deposition rate in a magnetron system. Insulating material are sputtered by RF sputtering since DC power results in electrical discharging due to surface charge accumulation at the target which produces poor quality film. Electrons are associated with ionization of the gas which are more mobile than ions and therefore respond and oscillate to follow the applied frequency. To maintain the plasma with an insulating target material such as BST, RF power supply is required because a prohibitively use of high voltage for DC sputtering to occur [Ohring *et al,* 1992]. This power supply usually operates in the 13.56 MHz, and is able of >100 W output power. A impedance matching network is requisite to match the output impedance to the input impedance of the RF magnetron system. Matching network is adjusted after establishment of RF plasma and the rejected power is minimised. Figure 3.5 shows the RF magnetron sputtering system located in Indian Institute of Technology, Jodhpur (IITJ) Laboratory.

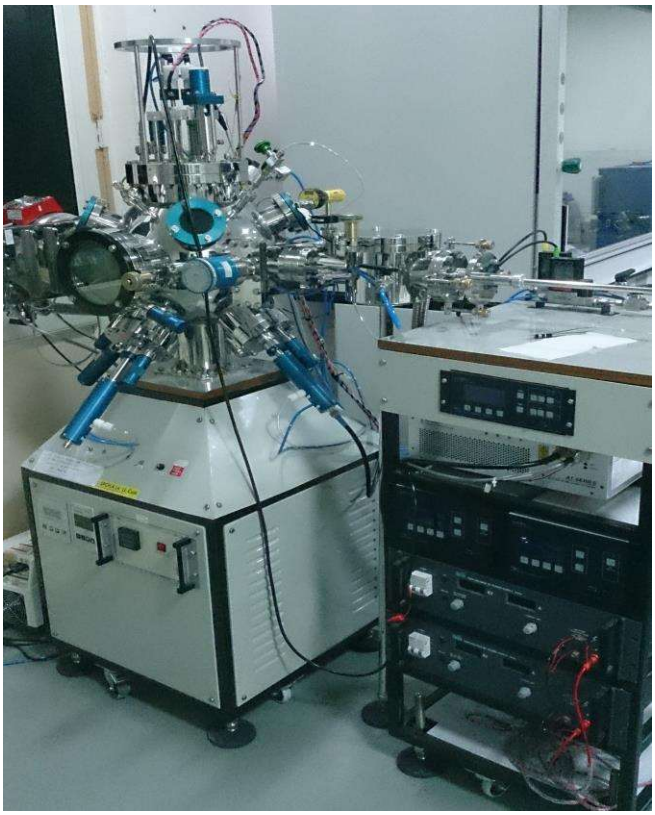

Figure 3.5: View of the RF magnetron sputtering system at IIT Jodhpur

50 mm diameter circular sputtering targets are configured to the magnetron with a stainless steel clamp. A proper arrangement is made to ensure good thermal contact between the magnetron and target. A water cooling system is attached to maintain the temperature of various mountings during deposition. Turbomolecular high vacuum pump and a rotary pump are part of RF magnetron system. After loading a sample on substrate position into the deposition chamber, roughing pump is used to bring the chamber pressure down to ≈ 2 mTorr. A turbomolecular pump (TMP) is used for both to achieve high vacuum and maintain suitable chamber pressure during film deposition. Material properties of sputtered film are influenced by various parameters i.e. RF power density (W/cm^2), sputter gas mixture, substrate temperature, substrate to target distance and working/sputtering gas pressure. Hence optimisation of deposition parameters is an essential requirement for each material deposition.

3.2.2 Pulsed Laser Deposition (PLD)

PLD has been considered as one of the suitable method for most oxide thin film growth and extensively used for growth of ferroelectric film [Zhu *et al,* 2005]. Physical processes are complex in PLD and interconnected, and governed by laser pulse parameters and target material properties. Small and intense laser pulses are used unlike sputtering to evaporate and ablate the target material. The laser ablates the target and thin film is produced by condensing the ablated material on the substrate surface. PLD technique is governed by the interaction between the solid surface and laser. This interaction mechanism involves (1) absorption of photon energy by the target material and heat conduction, (2) surface melting of target and (3) evaporation and ionization of oxide target. Radiating laser on the solid surface leads to conversion of the photon energy into electronic excitation and subsequently thermal, mechanical and chemical energy are generated which cause evaporation, plasma creation and ablation. When the extremely short laser pulses (20 ns) are incident on target surface, the surface temperature increases to thousands of degrees celsius by absorption of photons on the surface. A molten layer is formed on the surface while the bulk of the target material maintains room temperature. The involved mass transport is substantial in such short vaporization process and generates burst of evaporants that in turn produce thin film by deposition onto the substrate with the same composition of the target material.

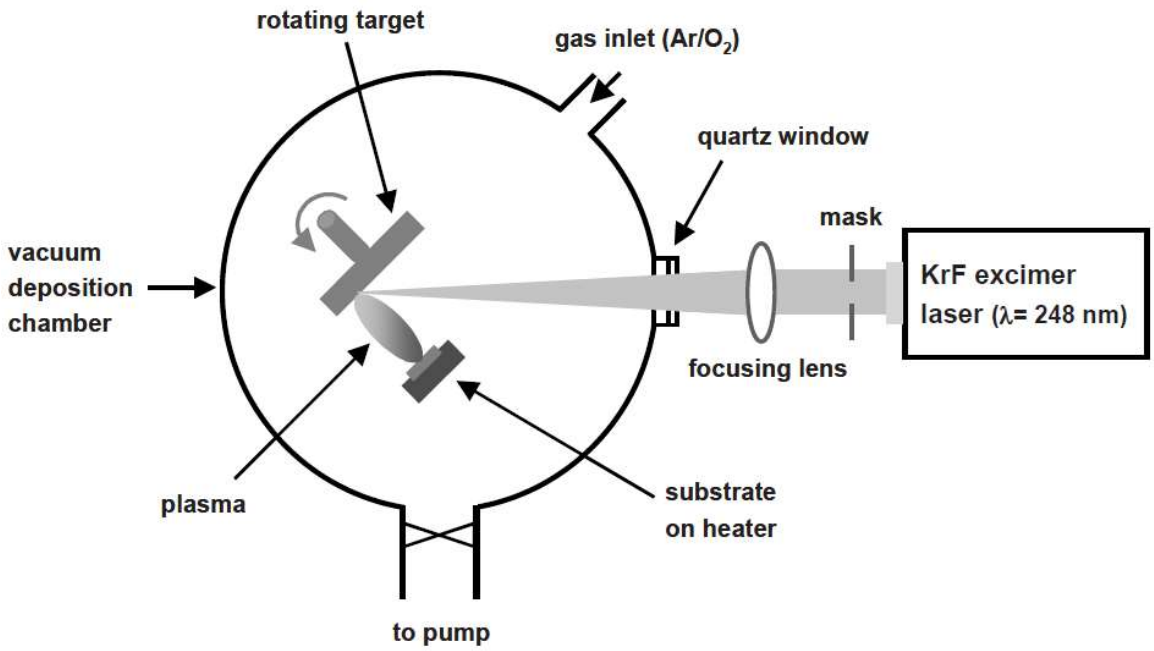

Figure 3.6. Schematic view of Pulsed Laser Deposition

A window, provided in deposition chamber is used to pass an intense laser and will be focused onto a target where it is absorbed to some extent. A supersonic jet of plume is formed to hit on the normal of the target. Significant removal of the material occurs in the form of a plume above a certain power density. The threshold power density required to generate such a plume are governed by material, morphology, laser duration and pulse wavelength. The constituents of the plume of evaporants are energetic species such as molecules, electrons, atoms, ions and solid particulates. The plume has a tight confinement of the evaporants and hence there is very less contamination when the evaporants are condensed on the substrate. The quality of films can be improved by increasing the surface mobility of the evaporants with increasing plasma temperature by the secondary interaction between the plume and the laser beam. The deposition can be done at higher oxygen pressure and crystallisation of the deposited film is feasible at comparatively low substrate temperature. The stoichiometry of the target material retains in deposited film. Oxygen as a reactive gas binds the volatile species to the substrate and support to conserve stoichiometry of the film. The high surface mobility help to produce oriented and crystalline films during deposition. Strong absorption of laser light also helpful to deposit the materials with high melting temperature. PLD has its drawback mainly with particulate formation. Targets with highly dense and smooth surfaces with proper substrate positioning are effective against particulate formation. Considerable care should be follow during rotation of the target to avoid crater formation and obtaining uniform erosion. The PLD system has an arrangement to keep energy source (laser) outside the deposition chamber, which allows more flexibility of ablation process in materials. Also growth rates may be controlled because of the pulsed nature of the laser beam. Moreover evaporating source material is confined to a small area close to the incident laser beam. Several deposition parameters have pronounced effects on the stoichiometry, deposition rate, material composition and crystalline quality of ferroelectric films. The parameters includes ambient gas pressure, substrate temperature, laser wavelength, laser spot size, fluence, substrate-to-target distance and target composition [Purice *et al,* 2006]. The schematic view of the PLD system is shown in Figure 3.6. The system is competent for deposition of multi- layer structures at various substrate temperatures with an arrangement to use partial pressure of argon, nitrogen and oxygen. Beam profile selection is made for better homogeneous energy density and plasma control with help of mask. The laser beam is projected by a lens through a chamber window and focused onto the target at an angle of 45^0. The laser spot size can be adjusted with lens and mask position in order of few square milimeter. The pressure inside the chamber is controlled using mass flow controller for flow rate of deposition gas. Temerature control is done by using proportional integral derivative (PID) temperature controller to adjust substrate temperature up to 900 ^{0}C.

3.2.3 Thermal Evaporation

Thermal evaporation deposition is a simple technique where a material is evaporated through heating the source that generates a sufficient flux of materials and deposited on a substrate. The films are grown under high vacuum condition where individual atomic species are delivered on to the substrate. During deposition, low growth pressure is required for delivery of a beam to avoid scattering processes. The main sub component of the physical evaporation systems is a high vacuum deposition chamber with a desired source. Source is generally placed at the bottom of the deposition chamber. Thermal evaporation was used to deposit Ni/Al/Au top metal electrodes over the ferroelectric thin films. The technique involves evaporating source through source boat under vacuum by applying a large current. Metals of high melting point, i.e. W and Mo are commonly used for evaporating the material. The evaporant vaporises through heating the source boat and condenses on a substrate. The amount of required heat is generated through the phenomenon of Joule heating to increase the temperature of the source boat or evaporant for evaporation. A SEMICORE thermal evaporator system was used for metal electrode deposition at IITJ as shown in Figure 3.7.

Figure 3.7: Thermal Deposition System

Source temperature could not be kept uniform because of heat dissipation through the electrodes. Therefore, in situ monitoring of the deposition rate is essential due to high variation unlike sputter deposition. The resonant characteristics of piezoelectric quartz are used to detect a vapour flux and amount of deposited material can be estimated based on vapor flux which ultimately gives thickness of the film. The substrate sample is kept at the same slope as the quartz crystal in such a way that fluxes from the source arrives at the sample simultaneously. The quartz wafer vibrating to its resonant frequency and generates an oscillating voltage. Metal electrodes act as electrical coupling which are on opposite faces of the wafer. One side of the wafer is exposed during the deposition to the vapour flux and mass accumulation happens. The accumulated mass consequently reduces the resonant frequency of the crystal and mass of the deposit film can be calculated with comparison of the amount of the reduced frequency to resonant frequency of reference crystal. The system is capable to achieve vacuum of below $9x10^{-7}$ Torr before the evaporation.

3.3 X-RAY DIFFRACTION

A crystalline substance performs as three-dimensional diffraction gratings for x-ray wavelengths comparable to the spacing of planes in the crystal lattice. X-ray diffraction is a common method to study the crystal structures and lattice spacing as shown in Figure 3.8. The x-rays are produced by a cathode ray tube and filtered to generate monochromatic radiations which are collimated to direct toward the sample. The principle is based on constructive interference of monochromatic x-rays and crystalline material for x-ray diffraction. The constructive interference is formed by satisfying the Bragg's condition ($n\lambda=2d\sin\theta$) during interaction of the incident rays with the sample. Bragg's law relates the diffraction angle and the lattice spacing in a crystalline sample to the wavelength of electromagnetic radiation.

The sample is scanned through a range of 2θ angles corresponding to all possible diffraction peaks of the lattice. These x-rays are directed toward the sample and diffracted rays are detected. The diffracted x-rays from the material are then detected, processed and counted. Identification of the material is carried out by conversion of the diffraction peaks to d-spacings, since each material has a set of unique d-spacing. The identification is done with comparison of d-spacings to a standard reference patterns. A crucial part of all diffraction measurement is the angle between the incident and diffracted rays.

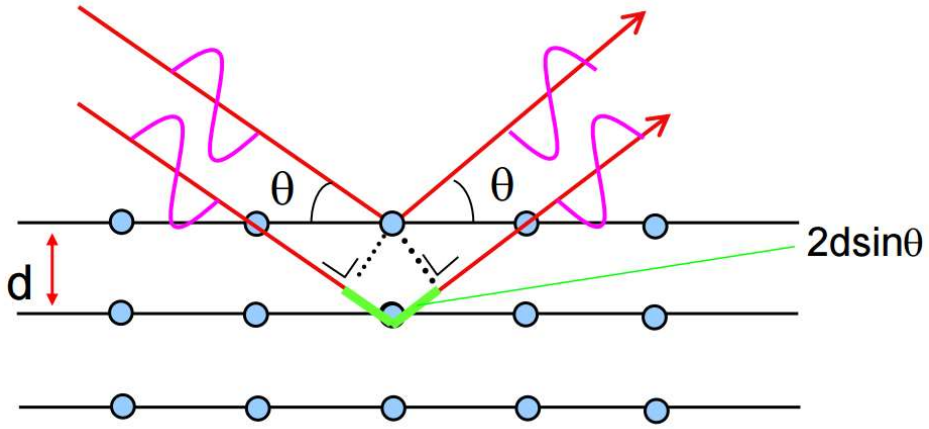

Figure 3.8: X-ray diffraction process

X-ray diffractometer system consists of three basic componenets: x-ray tube, x-ray detector and sample holder. X-rays are produced in a cathode ray tube by heating a filament to generate electrons which are accelerated by applying a suitable voltage toward a target, and bombarding the target material. Characteristic x-ray are produced if the electrons have enough energy to eject out inner shell electrons of the target material and a spectra is obtained. These spectra consist of many components and the most common are K_α and K_β. The specific wavelengths, produced from x-ray tube are characteristic of the target material (Cu, Mo, Fe). Monochromatic X-rays are needed for diffraction by filtering with help of crystal monochromator or foils. Copper is the most common target material for crystal diffraction, with x-ray wave length of 1.5418 A^0. The intensity of the reflected x-rays is recorded when detector is rotated around the sample. When the geometry of the incident x-rays and the sample follows the Bragg's Equation, constructive interference formed and an intense peak is observed. The geometry of an x-ray diffractometer is shown in Figure 3.9. The detector rotates at an angle of 2θ to collect the diffracted rays from sample while the collimated x-ray beam incident at an angle of θ.

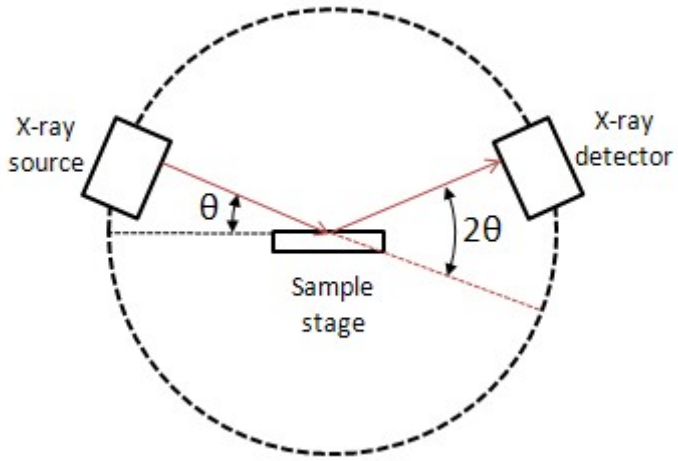

Figure 3.9: 2θ-ω measurement from X-ray diffraction

A detector accounts and processes this x-ray signal and provides output to attached computer. The intensity of diffracted x-rays is constantly recorded during the process when the detector rotates through their relevant angles. Results are usually presented in form of peak positions (2θ) and x-ray counts (intensity). The d-spacing of each peak is then calculated by condition of the Bragg's law for the fitting value of λ. The d- spacing is correlated with h,k,l plane and by comparing with available literature data, material identification is carried out.

3.4 ATOMIC FORCE MICROSCOPE

An atomic force microscope (AFM) is used to observe changes in surface morphology of thin film surface. The AFM probes the surface of a sample with a sharp tip of few Å in diameter, is located at the free end of a cantilever. The spring constant of cantilever is lower than the effective spring constant which holds the atoms of the sample together. When the scanner smoothly traces the tip across the thin film, the contact force causes to bend the cantilever or deflect, to accommodate changes in topography. A position sensitive photo detector (PSPD) is used to measure a deflection in the cantilever when the sample is scanned under tip. The deflection sensor is based on the principle of beam bounce technique where reflecting a laser beam off the back of the cantilever onto a photo detector. Position of the laser spot shift on the detector when the cantilever bends. The shift in the position is quantitative measurement of deflection in the cantilever. Therefore map of surface topography is generated from the measured cantilever deflections. For proper operation of AFM the intensity of the reflected beam must hit the PSPD whereas laser spot must hit the cantilever tip and both must be above a definite level. The schematic of the AFM components is shown in Figure 3.10.

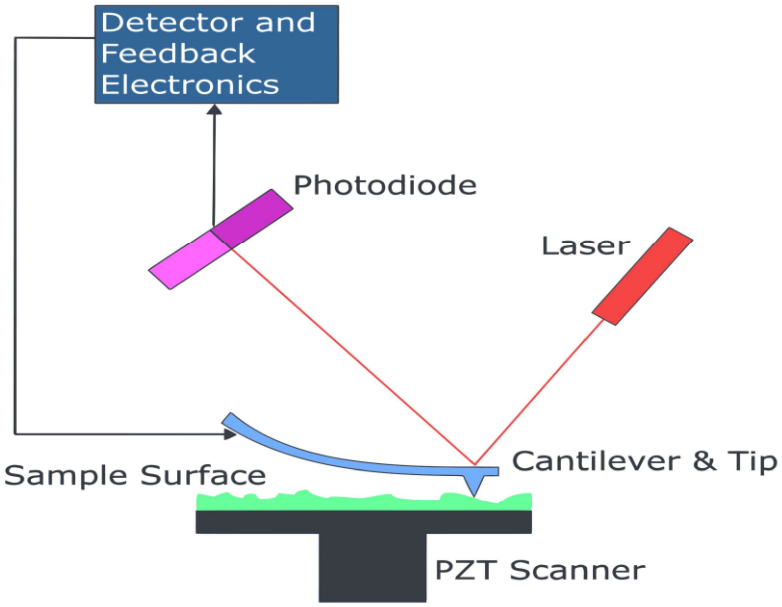

Figure 3.10: Schematic representation of Atomic Force Microscope

There are two modes of AFM operation i.e. contact mode and non contact mode. The tip to sample distance is less than a few angstroms in contact mode while tip to sample distance ranges from 10-100Å in a non-contact mode. Non contact mode works under attractive regime in respect of inter atomic force between the samples and tip whereas the contact mode works under repulsive regime. Further, contact mode AFM is performed in two different modes which include constant-height mode and constant force mode. Constant force mode is usually applied to capture images of large and irregular regions of the sample surface. Images are recorded with feedback enabled and set to a modest value. The 'z' position of the scanner is controlled by the signal from the feedback loop to maintain a constant force by extending or retracting the tip to

control the tip to sample spacing. The 'z' directional motion of the scanner matches with the surface morphology of sample after optimising the feedback parameters. The topography signals are signal from the feedback loop are used to produce an image of the surface. Constant-height mode is normally used to take images of smaller and smoother regions of the surface with higher resolution in atomic resolution. The 'z' feedback is kept minimal by setting low gain and consequently the force on the cantilever, the sample's topography and surface electronic structure. Hence, the difference between the set value and probe signal, referred as error signal, can be used to create an image of the surface. The tip to sample spacing is not changed with minimal feedback which maintains a constant probe signal in constant-height mode. The images are obtained faster than the constant-force mode since feedback is minimized which reject the time lag for response of the feedback loop. Constant-height mode can only be applied to record images of smooth surfaces because of constraint for movement of scanner in 'z' position thus changes in surface topography cannot observed.

Non-Contact mode of operation is based on the correlation between the cantilever resonance frequency and topography to produce the image. Each cantilever has its characteristic resonant frequency, which is linked to the tip dimension and material. The non contact mode is an indirect measure of sample topography by using detection of a cantilever's resonant frequency. There is always requirement for providing a way of measuring sample topography with small contact or without contact between the tip and sample. The applied force is very low between the tip and the sample which is advantageous for elastic samples. The cantilevers used for non contact mode must be stiffer than contact mode to avoid attraction by sample surface.

Conductive AFM mode is one of powerful current sensing technique which are used for the conductivity variations in resistive samples. The conducting mode may help to investigate the electrical properties and to reveal local conductivity fluctuation in thin films. The current measurement can be performed in the range of hundreds of femto amperes to micro amperes. Conductive mode can simultaneously map the topography and current distribution of a sample. This mode is helpful in a wide variety of material characterization including thin dielectric films, nanotubes etc.

3.5 X-RAY PHOTOELECTRON SPECTROSCOPY

The x-ray photoelectron spectroscopy is based on principle where energy distribution of the ejected photo-electrons is measured and the surface chemical states and relative concentration of elements can be determined. In photoelectron spectroscopy, photoelectric effect is the process of prime importance for the interaction of the electromagnetic wave. Photo electrons are emitted from the cloud of core electrons during the photo electric process. Valence electrons which is responsible for the binding of atoms together in molecules and solids. Magnitude of the kinetic energy of emitted electron is dependent upon both binding energy of core electron and the incident photon energy. The kinetic energy measurement of the emitted photoelectrons is an essential part of photoelectron spectroscopy. However interaction of radiation with matter can excite to its higher energy, generally named as excited state which is a meta-stable state. The atom or a molecule in its meta-stable state can relax through different process such as luminescence, dissociation, degradation to vibrational energy and electron emission by losing excess energy to reach ground state. Thus emitted electrons in other process are different from that of photoelectrons and are alternatively known as pre-ionization or auto-ionization. When monochromatic x-ray beam incident on the sample, it gets absorbed by one of the atoms and give rise to emitting photoelectron. The binding energy can be determined as:

$$E_B = h\upsilon - E_K - \varphi \tag{3.4}$$

where E_B refers binding energy of photoelectron, $h\upsilon$ is energy of incident x-rays, and φ is dependent on both material and spectrometer. The information of the energy of the monochromatic photon and the measurement of the kinetic energy of the photoelectron will

give the binding energy of the emitted core electron. This binding energy is the characteristic of an atomic species in form of its chemical state and co-ordination among the neighbouring species. The binding energy of valence electrons would be less as compared to the core electrons due to the screening effect by core electron cloud. The auto ionisation could prevail over the probability of photoelectron emission due to presence of excited state which matches with the energy of absorbed photon. Therefore, it is necessary to avoid the photon energies which match with the absorption levels of the solid. This could be achieved in practice by using a photon beam of energy greater than 10-20 eV, using either x-ray or UV source. In the process of photoelectric effect, generation of a photoelectron occurs by the ionization of the absorbing site and followed by interaction of photoelectron with the other atoms and its emission into the vacuum.

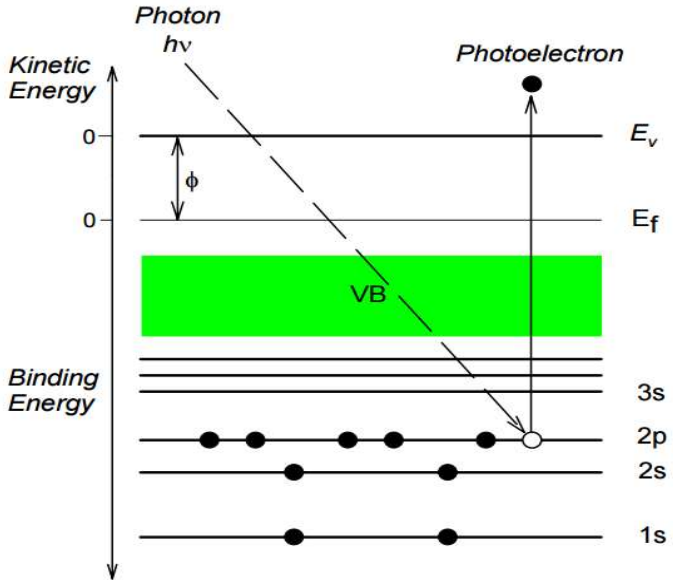

Figure 3.11: X-Ray Photoemission process

The emitted photoelectrons from the depth d with initial intensity I_0 and intensity I_S at the surface after attenuation by the material can be described by Beer Lambert law:

$$I_S = I_0\, e^{-d/\lambda} \tag{3.5}$$

where λ is inelastic mean free path of an electron.

The sampling depth is defined as thickness at where 95% of photoelectrons are scattered before reaching to the surface and achieved at a depth of 3λ. Inelastic mean free path is governed by kinetic energy of the photoelectron and material. The mean free path 'λ' is around 1-3 nm for Al K_α radiation which gives sampling depth of 3-10nm. The binding energy of the electrons is different in the atomic species for different oxidation states. The binding energy of a core electron is lower for a neutral atom than that of an ion. Hence, the peak observed in the binding energy corresponding to an elemental in ionic state is generally higher than that observed for that of the same element. This can be attributed because of the enhanced attraction of the nucleus over the core electron in the ionic state. Splitting in the observed core level spectra are produced by presence of spin orbit coupling in the ions which gives rise to doublets. These doublets are useful signal of the oxidation state of a multivalent cation. Each atom in the surface has core electrons with a definite binding energy and the core level shift gives information about the chemical bonding and valence states in a thin surface layer [Ohring, 1992]. The X-ray Photoelectron Spectroscopy (XPS) measurements carried out for this study was performed using Al K_α radiation (1486.60 eV).

For insulating samples such as BST, a positive charge zone is formed on the surface when the photoelectrons are ejected out from the surface. The positive potential may vary from few volts to tens of volts which results a shift in the XPS peak position. The binding energy of adventitious carbon, C1s peak with a typical binding energy from 284.6 - 285.0 eV is used in such a case, as the calibration reference. A low-energy electron flood gun can also be used sometime to deliver the electrons into the sample, in turn neutralise the surface charge. The core electron of any atom has a unique binding energy, like a "fingerprint" which is susceptible to the chemical environment of the atom. The core electron of an atom can exhibit a change in the binding energy due to its bonding to different chemical species which result to shift of the corresponding XPS peak, called the chemical shift. The measurement of chemical shift is helpful to identify the chemical state of surface elements [Reinert and Hüfner, 2005], which might be ranging from 0.1 eV to 10 eV. XPS has been proven as an important technique to study the near surface/interface chemistry of $ATiO_3$ compositions in thin film [Li *et al,* 2005] and bulk. However, the near surface/interface chemistry of perovskite titanates structure (ABO_3) was not understood properly. When an electrical contact is made during the measurement between the sample and the spectrometer, their respective Fermi energies will be aligned and considered as reference for the recorded binding energies. This will be used to estimate the position of the Fermi level (E_F) due to changes in chemical, coordination number and strain in the material. There are three types of measurements can be performed during the surface analysis which includes (i) the survey spectrum to identify all the chemical elements at the surface, (ii)core levels spectra at their characteristic binding energies and (iii) the valence band spectrum to know the position of Fermi level. The valence band maxima (VBM) of the spectra are calculated by linear extrapolation of the principal edge of the valence band emission.

3.6 UV-VIS-NIR SPECTROPHOTOMETER

Optical characterisations of thin films are related to physical phenomenon like reflection, transmission and absorption. Two light sources are used in Ultra Violet -Visible-Near Infrared (UV-VIS-NIR) spectrophotometer i.e. a deuterium lamp for ultraviolet region and halogen lamp for visible and NIR region. The source light progressed being reflected from mirror and passes through slit to reach at diffraction grating. The grating is being rotated to allow for selection of a specific wavelength and only monochromatic beam passes through another slit at any specific grating orientation. Unwanted higher order diffracted beams are removed by using a filter. One of the beams is passed through a reference sample whereas the other beam passes through the sample with film coated on substrate. Thereafter intensities of the light beams are recorded and transmittance is obtained by the ratio of the sample signal to reference signal (I/I_0). The measured spectral transmittance is useful to obtain important parameters which include optical band gap, thickness and refractive index.

In the region of strong absorption, Beer-Lambert's law given as follows:

$$I=I_o \exp(-\alpha d) \tag{3.6}$$

where, I= intensity at a given wavelength 'λ', Io= incident intensity , d is the thickness of the film and α the absorption coefficient in cm^{-1}. The absorption coefficient α can be calculated whereas I is the measured transmission. The absorption edge of the film can be calculated by knowing α, from Tauc's expression.

$$\alpha h\upsilon = \text{constant } 'x' (h\upsilon - Eg)^2 \tag{3.7}$$

Band gap of the material will be obtained by plot of $(\alpha h\upsilon)^{1/2}$ vs $h\upsilon$ with extrapolation of the linear region at the intercept of X axis.

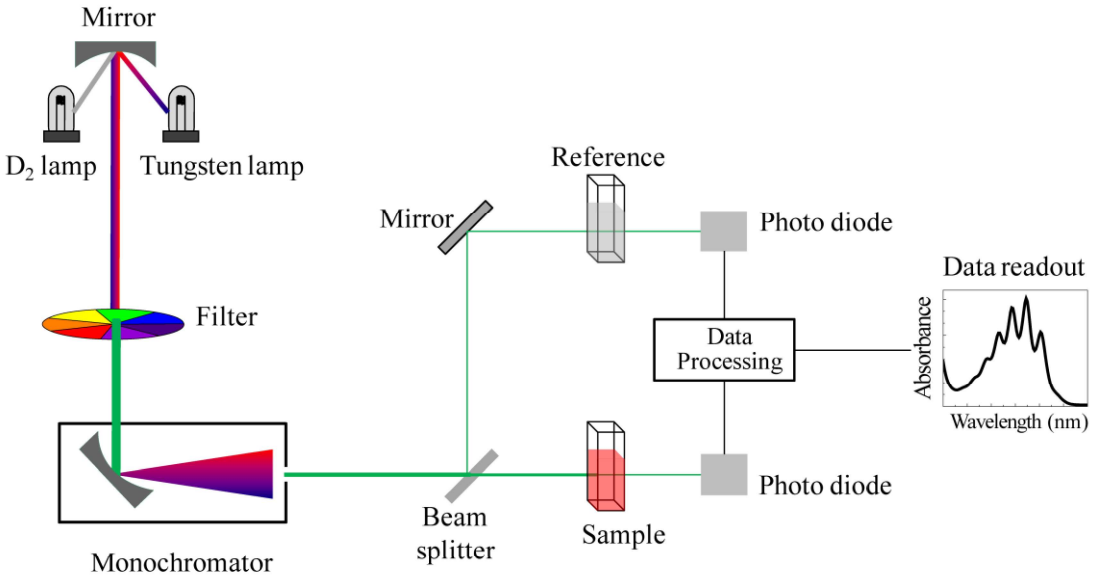

Figure 3.12: Schematic illustration of Optical Characterisation process
(Source: https://commons.wikimedia.org/wiki/File:Schematic_of_UV-_visible_spectrophotometer)

3.7 PEROVSKITE THIN FILMS FOR MICROWAVE CIRCUIT APPLICATIONS

Tunable microwave devices based on thin films generally rely on varactors as the tunable circuit component. A set of electrodes is required to fabricate varactors from thin films, connecting the component to the external circuit and apply bias field. In most cases, a single set of electrodes serves both purposes simultaneously. Metal-insulator-metal devices (MIMs) and Interdigitate Capacitors (IDCs) are the two types of configuration which are used to measure the capacitance of a thin film.

3.7.1 Interdigitated Capacitor (IDC)

An IDC structure is shown schematically in Figure 3.13 and is patterned by depositing dielectric films on the suitable substrate followed by interdigitated electrode metallization on top. IDCs are simpler to manufacture compared to parallel plate configuration which necessitate more masking process steps. Interdigitated capacitors do not have issues related to chemical and mechanical stability of the bottom electrode under film growth condition and reduces microstructural degradation at interface. IDCs can handle higher breakdown voltages. Tunability of the device can be increased at lower voltage by reducing finger spacing.

Figure 3.13: Schematic view of Interdigitated Capacitors

A high power phased array antenna application uses the properties of higher breakdown whereas easier fabrication steps make it attractive for low cost circuit applications. The dielectric constant of the perovskite film is tuned by applying a DC bias between the interdigitated electrodes. The interdigitated electrodes should be patterned from a highly conductive metal (Cu or Au) to minimise the losses. The relative permittivity of the film measured in the IDC configuration is dependent on the dimensionless parameters for the film thickness and the electrode width.

3.8.2 Parallel Plate Capacitor

Parallel plate structure is fabricated in form of MIM configuration by depositing the film straight on bottom electrode and top electrodes are patterned over the dielectric layer. The distance between the electrodes is taken as equal to film thickness which is much smaller than finger spacing in interdigitated structures. A schematic diagram of a parallel plate capacitor is shown in Figure 3.14.

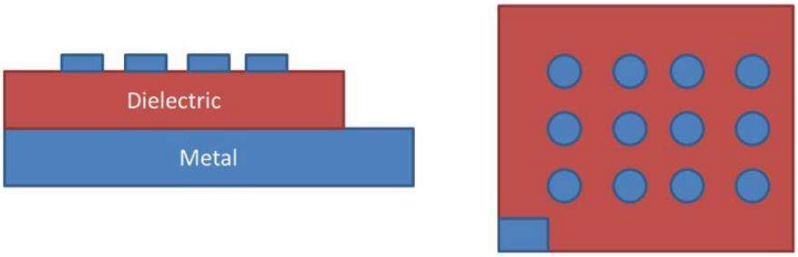

Figure 3.14: Schematic of Parallel Plate Capacitors

3.9 ELECTRICAL CHARACTERISATION

Analysis of electrical properties in thin films is of higher importance in terms of fundamental and application aspects. The leakage current conduction plays important role in the ferroelectric thin films. The leakage currents decide performance of device and the dielectric breakdown of the thin films. It limits the operational functionality of the device, with respect to the applied field, radiation environment and dimension of the thin film. The presence of grain boundaries, defects, and electric potential barriers at the film-electrode interfaces dominate over the actual bulk current conduction phenomena in thin films. The leakage current analysis has always been essential requirement for many applications to ensure very less flow of charge through the dielectric material. The frequency and voltage dependent dielectric properties of films were characterized using SCS 4200 Kiethley Systems (Figure 3.15) at low frequencies (≈ 1MHz) using the MIM structures.

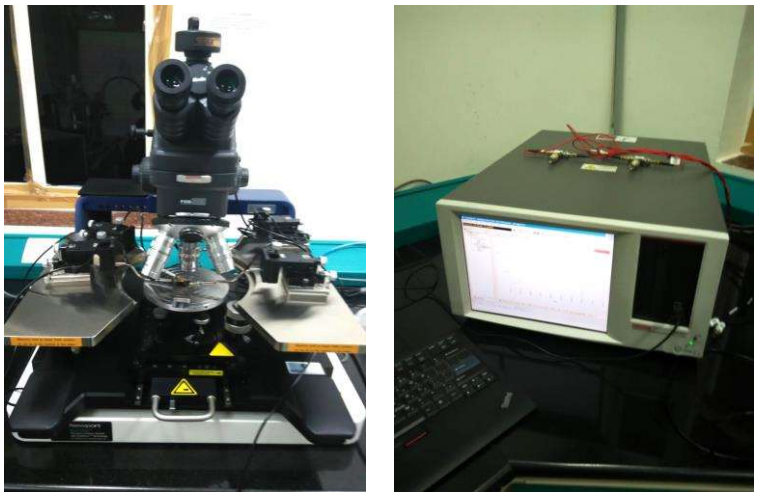

Figure 3.15: Kithley SCS 4200 electrical measurement systems

Apart from the polarization measurements the capacitance-voltage (C-V) measurements has been considered a possible way to study the ferroeletcric (FE) characteristics of a material. C-V behavior of FE material is known to mimic the slope of the polarization-electric field (PE) curve but not exactly the slope due to variation in the measurement conditions [Dawber *et al,* 2005]. Electrical measurements were carried out using both IDC and parallel plate capacitor on top electrode patterned perovskite ferroelectric thin films.

Capacitance and tanδ have been measured over a range of DC bias superimposed on the sinusoidal voltage signal. The recorded *C-V* data permits calculation of the dielectric loss and tunability of the BST film at different DC bias. Dielectric frequency dispersion was measured using the same set-up that is used for C-V characterization. Capacitance versus DC bias yields a quantitative assessment of loss tangent, tunability and the ability to tolerate high fields. The electrical characterization experiment allows an acceptable understanding of the dielectric properties of thin films which relate to tunable varactors in frequency-agile devices.

3.10 HIGH ENERGY IRRADIATION

There were two radioactive source were used for high energy radiation and exposure was given to the samples separately. ^{60}Co source was selected for high energy gamma irradiation wheras ^{252}Cf for neutron irradiation.

3.10.1 Gamma Irradiation

The gamma irradiation facility contains ^{60}Co radioactive source as shown in Figure 3.16. The facility has several cylindrical dry tubes that contain ^{60}Co pencils in a circular configuration. Sample chamber is surrounded by the ^{60}Co pencil and sample is kept in the chamber. This whole arrangement is covered by optimum lead shielding to avoid radiation exposure. The irradiation facility is controlled through control mechanism and sample can be put inside the chamber with motor controlled operation. The sample is exposed from the radiation from all sides during irradiation. The dose rate can be read from the display panel and accumulated dose can be calculated for specific time period.

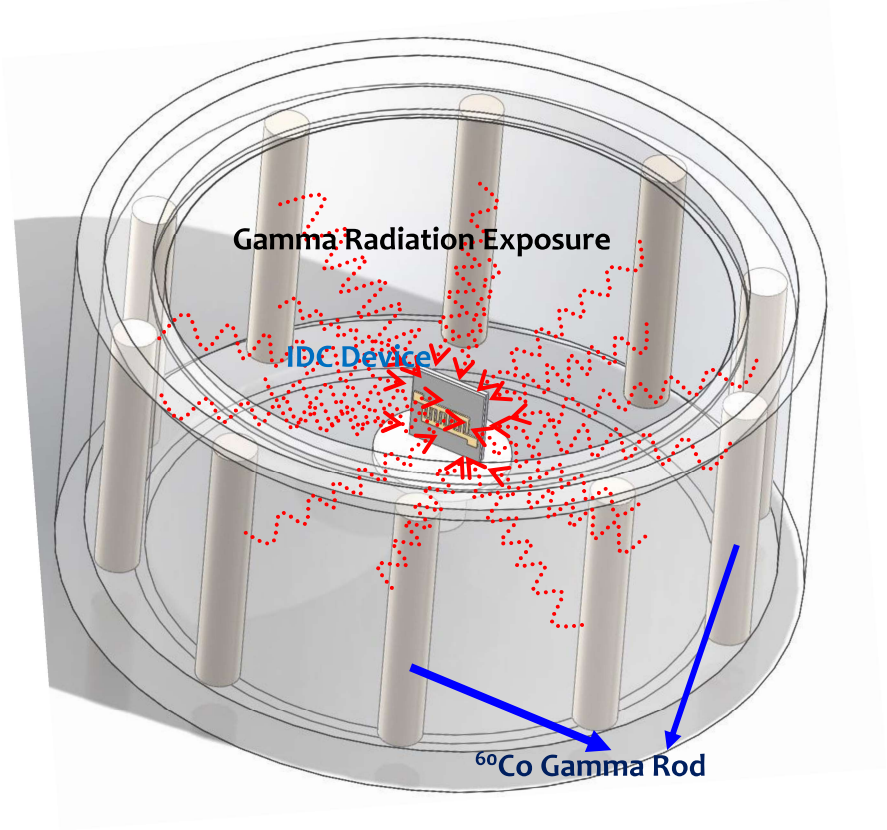

Figure 3.16: Schematic representation of gamma irradiation

3.10.2 Neutron Irradiation

The neutron irradiation experiment was carried with the ^{252}Cf neutron source. A vertical irradiation arrangement is made for sample irradiation as demonstrated in Figure 3.17. The neutron source is kept in cylindrical tube and inside the shielded enclosure. This cylindrical tube is raised up while the sample is irradiated. The sample is typically mounted 6 cm away from the source position during the irradiation. The samples were wrapped inside a small plastic to avoid dust etc.. The thin film samples were exposed for different time period to attain different neutron fluences.

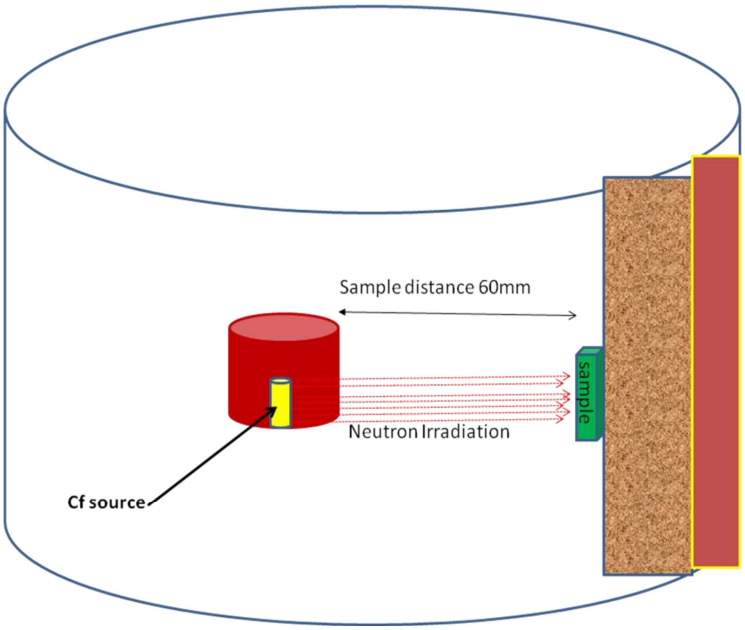

Figure 3.17: Schematic representation of neutron irradiation